physica status solidi rrl

www.pss-rapid.com

Bi-Stability of Magnetic Skyrmions in Ultrathin Multilayer Nanodots Induced by Magnetostatic Interaction

M. Zelent, J. Tóbik, M. Krawczyk, K. Y. Guslienko, and M. Mruczkiewicz**

We report the results of simulations of magnetic skyrmion stability in ultrathin magnetic multilayer nanodots with interfacial Dzyaloshinskii–Moriya exchange interaction (DMI). We found that in presence of the lateral confinement the magnetostatic energy significantly influences the skyrmion stability and leads to stabilization of large-radius skyrmion even at low values of the DMI strength, in addition to small-radius skyrmion stabilized by DMI. In particular, stabilization of the skyrmion state with two different radii (bi-stability) is found in dipolarly-coupled $(Pt/Co/Ir)_n$ circular nanodots with the number of repeats of the unit cell $n = 3$ and 5. The bi-stability range is located at the DMI strength of 0.9–1.1 mJ m^{-2} or at the total Co-layer thickness of 2.2–2.6 nm.

Magnetic skyrmions are topologically non-trivial inhomogeneous magnetization configurations that can be stabilized in thin ferromagnetic films or non-centrosymmetric bulk magnetic crystals. The strong spin–orbit coupling and lack of the inversion symmetry give rise to the chiral Dzyaloshinskii–Moriya exchange interaction (DMI),[1,2] such as in bulk helimagnetic materials with cubic B20 crystal lattice (bulk DMI), or at the interface between two dissimilar materials, ferromagnet/heavy metal (interfacial DMI).[3,4] Both types of DMI are considered to be favoring the chiral skyrmion stabilization, either in ground state (the lowest energy state) or metastable state (a higher energy local energy minimum). The skyrmion classification in uniaxial magnets according to the crystal symmetry was suggested on the base of Lifshitz invariants, see Ref. [5] and references therein. The cubic DMI typically leads to stability of a Bloch skyrmion, where magnetization rotates perpendicular to radial direction moving away from the center of the skyrmion. Whereas, uniaxial interfacial DMI increases the stability of a Néel skyrmion (**Figure 1**a), where magnetization rotates in the plane parallel to radial direction. Nanosize skyrmions have a potential to provide useful solutions for cheap low-power, high-density data storage, and processing.[6–10] The discovery of strong interfacial DMI in ultrathin Co/Pt, Co/Pd, and Co/Pt/Ir multilayer films and dots expanded the possibilities for individual skyrmion stabilization in nanostructures.[11,12]

Moreau-Luchaire et al.[11] observed by scanning transmission X-ray microscopy stable sub-100nm magnetic skyrmions in dipolarly-coupled Pt/Co/Ir multilayers. Boulle et al. observed the Néel skyrmions in Pt/Co/MgO dots by photoemission electron microscopy combined with X-ray magnetic circular dichroism. [13] Recently, Pollard et al.[12] reported on Lorentz microscopy imaging of less than 100nm stable skyrmions in exchange-coupled Co/Pd multilayers at room temperature. The stability of an isolated skyrmion in infinite film applying perpendicular magnetic field was discussed in Refs. [5,9]. Very recently two types of skyrmions or bubbles with different radii were found to be stable in some cases in infinite ferromagnetic film.[14] Starting from Ref. [15], the skyrmion triangular lattices in bulk ferromagnets and infinite films were intensively investigated.[16] It was shown that lateral confinement modifies the conditions for the skyrmion stability significantly in ultrathin films,[10,13,17–23] as well as in the case of the B20 compounds.[17,18,24]

Recent studies demonstrated that the magnetic skyrmions are promising candidates for solving problems with unstable data storage, when size of the memory unit cells is decreasing below a critical size resulting in data loss.[25,26] It was shown that the skyrmions with opposite core polarities reveal hysteresis behavior when external magnetic field is varied.[6] This feature is of interest to design a new generation of data storage devices. In Ref. [19] the stability of a Néel skyrmion in circular nanodot was studied, and it was shown that due to the dot edge presence, the skyrmions with the sizes R_s/R (R_s is a skyrmion radius) between 0.50 and 0.78 are stable above critical value of DMI, D_c, for the dot radii $R = 25$–100 nm. In this study, the magnetostatic interaction was accounted as an effective uniaxial magnetic anisotropy.

However, increasing the dot thickness the magnetostatic energy is expected to play an important role in skyrmion stabilization even in ultrathin films/dots and should be taken into account.[13,21,27] It might even lead to stabilization of antiskyrmions with no DMI.[28]

M. Zelent, Prof. M. Krawczyk
Faculty of Physics, Adam Mickiewicz University in Poznan, 61-614 Poznań, Poland
E-mail: mateusz.zelent@amu.edu.pl

Dr. J. Tóbik, Dr. M. Mruczkiewicz
Institute of Electrical Engineering, Slovak Academy of Sciences, 841 04 Bratislava, Slovakia
E-mail: m.mru@amu.edu.pl

Prof. K.Y. Guslienko
Depto. Fisica de Materiales, Universidad del País Vasco, UPV/EHU, 20018 San Sebastian, Spain

Prof. K.Y. Guslienko
IKERBASQUE, the Basque Foundation for Science, 48013 Bilbao, Spain

DOI: 10.1002/pssr.201700259

 © 2017 WILEY-VCH Verlag GmbH & Co. KGaA, Weinheim

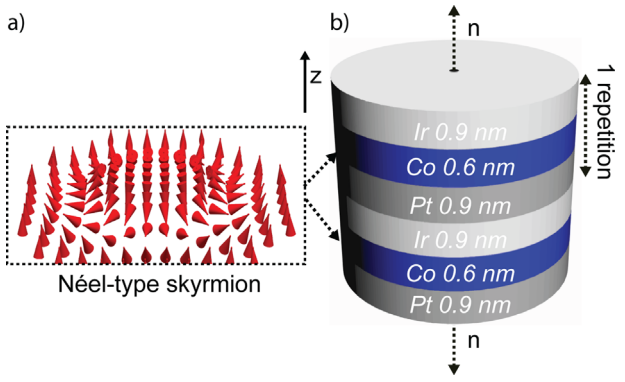

Figure 1. a) Magnetization configuration of the ferromagnetic layers in the circular layered dot (Néel-type skyrmion). b) Sketch of the multilayer nanodot based on dipolarly coupled ultrathin Co layers with varied number of repeats, n, of the Ir/Co/Pt unit cell.

The present paper is aiming at the following main points: Firstly, we show how the lateral confinement and corresponding magnetostatic energy lead to stabilization of the large-radius skyrmions, if DMI strength is weak. Secondly, we show that due to the lateral confinement and strong magnetostatic interactions, the skyrmions can be bi-stable in multilayer circular dots even at zero magnetic field.

A Néel skyrmion can be stabilized in a ultrathin dot within a finite range of interfacial DMI values, D. This range depends on competition of the DMI, exchange, anisotropy and magnetostatic interactions. The control of the magnetostatic interaction is realized by changing the number of repeats, n, of the Co layers in the stack (Figure 1). For a description of the skyrmion we use the reduced magnetization components $\boldsymbol{m} = \boldsymbol{M}/M_s = (m_r, m_\phi, m_z)$ in the cylindrical coordinate system with the z axis directed along the dot thickness.

Figure 2 shows the normalized skyrmion radii R_s/R for $n = 1$–9 repeats of the ferromagnetic layer of thickness $t_{Co} = 0.6$ nm, with Co–Co separation 1.8 nm, dot radius $R = 250$ nm and magnetic parameters corresponding to Pt/Co/Ir dot as given in Computational Details. The static skyrmion configurations were simulated with the procedure described in Computational Details. All considered skyrmions possess the same core polarity, m_z at the center of the dot, it is -1.

We can distinguish two types of skyrmions, small size and large size or bubble skyrmions, depending on DMI strength D (Figure 2a). The clear border between the skyrmions cannot be defined and in some cases there is continuous transition between these two types of the skyrmions when DMI strength is varied, for example $n = 1$ (red line in Figure 2a). We note that there is strong influence of the number of ferromagnetic layer repeats on the large radius skyrmion stability and size, evidencing that the magnetostatic interaction plays an important role in stabilization of this skyrmion. The smaller skyrmion can nucleate at the DMI strength above 0.92 mJ m^{-2} and the range where it can exist decreases as the number of repeats increases. The points marked as D_{Cn} indicate the edges of stability of the small radius skyrmions and inflation points for rapid grow of skyrmion size with increase of the DMI strength for each number n of ferromagnetic layers in the stack. Increasing

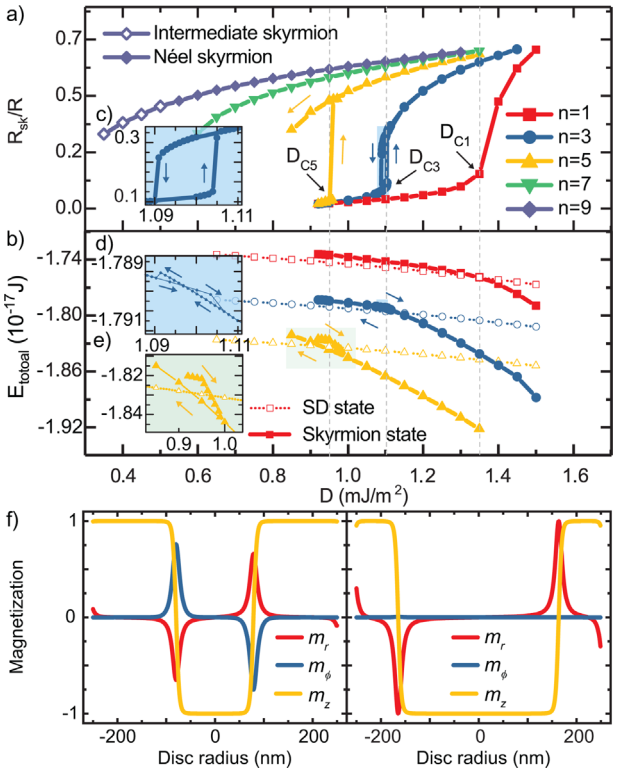

Figure 2. a) Normalized skyrmion radius, R_s/R, as a function of DMI strength D for different number of the ferromagnetic layers in the stack. D_{Cn} represents the edge of stability of the small radius skyrmion and inflection point for rapid grow of skyrmion size with increase of DMI. b) Total magnetic energy (including the DMI, exchange, anisotropy, and magnetostatic energies) for an isolated skyrmion (solid line), and for perpendicular single domain (SD) states as a function of DMI strength D for different numbers of the ferromagnetic layers. c) Inset: enlarged dependence of the skyrmion radius for $n = 3$. d,e) Inset: enlarged dependence of the total magnetic energy for $n = 5$ and 3 respectively. f) Profiles of the skyrmion magnetization components for $n = 9$ layers, at $D = 0.35$ mJ m^{-2} (on the left) and $D = 1.3$ mJ m^{-2} (on the right), plotted along the radial x direction.

number of repeats decreases the critical DMI value where stable small radius skyrmion starts to grow. Thus, we conclude that the increase of magnetostatic interaction strength leads to decreasing the stability range of the small radius skyrmion.

Increasing number of repeats extends the range of DMI where large radius skyrmions can be nucleated. However, the large DMI strength supports Néel-like skyrmion stabilization. Skyrmions with weak DMI strength lose the Néel-like character (the considerable m_r magnetization component resulting in extra magnetostatic energy[29] cannot be compensated by DMI), intermediate states between Bloch- and Néel-like skyrmions appear (Figure 2f), indicated by open dots in Figure 2a.[10] Therefore, the hysteresis is a competition between small radius Néel-like skyrmions and large radius skyrmions having non-zero m_ϕ magnetization component (intermediate Bloch/Néel skyrmions[10]). Further increase of the number of ferromagnetic layer repeats and magnetostatic interaction strength in the layered stack leads to stabilization of the Bloch-like skyrmions even at zero DMI.[21]

© 2017 WILEY-VCH Verlag GmbH & Co. KGaA, Weinheim

It was simulated (see Figure 2a) that in some range of DMI and for certain number of the layer repeats, there is bi-stability of skyrmion with the same core polarity, but different sizes. For single layer ($n = 1$) the bi-stability was not observed, however, it is present for 3 and 5 layers ($n = 3, 5$). The difference between the large and small skyrmion radii, at the same DMI value, is relatively small for 3 layers (for $D = 1.1\,\mathrm{mJ\,m^{-2}}$), but it increases for 5 layers (for $D = 0.95\,\mathrm{mJ\,m^{-2}}$), and is 75.5 and 114.3 nm, respectively. Further increasing the number of repeats leads to destroying of small-radius Néel skyrmion stability. Therefore, the bi-stability can be observed only if magnetostatic interaction has intermediate strength competing with DMI. For three layers ($n = 3$) we performed additional simulations, varying the dot radius R between 100 and 1000 nm. We found that there is a critical value of R that can support the skyrmion bi-stability and it is enhanced for large R. The range of D where bi-stable skyrmions can exist expands with increasing the dot radius.

As shown in Figure 2b the total magnetic energy (including the DMI, exchange, anisotropy, and magnetostatic energies) drawn as a solid line is higher than the single domain state energy for smaller skyrmion for each case. At higher values of D, the single domain state is no longer ground state, whereas the large radius skyrmion is. It is consistent with the previous observations.[30] For the cases $n = 7$ and $n = 9$ the energy of the large skyrmion is still lower than the SD energy.

Stable skyrmions with different equilibrium radii can be characterized by their relative energies and energy barrier separating them, see **Figure 3**a. To investigate the origin of two minima in the energy profile, we have analyzed the total energy and forces (and their components) acting on the skyrmion when the radius is varied at fixed DMI, $D = 0.95\,\mathrm{mJ\,m^{-2}}$. In order to plot the energy profile as a function of skyrmion radius $E(R_s)$, we use the frozen spins technique (see Computational Details). Since the DMI is strong enough to ensure the Néel type magnetization twisting, we assume that the frozen spins $m_z = 0$, $m_r = 1$ correspond to the lowest energy state at each radius of the ring, so the change of radius crosses a saddle point in the energy function and allows us to estimate the minimum energy path and height of the energy barrier for bi-stable skyrmions.

We replace multilayer dot with simplified system, a single-layer circular dot with effective Co thickness, t_{Co}. That allows to continuously change the magnetostatic contribution to the total energy and study its influence on the skyrmion stabilization. Specific t_{Co} could be also reproduced by a multilayer system with fitted t_{Co} and Co–Co layer separation[1]. Figure 3c presents simulated sizes of stable skyrmion states in the nanodot as a function of the layer thickness, t_{Co}. Simulations showed that bi-stability exists and two possible skyrmion states are stable within the range of Co thickness 2.2–2.6 nm.

When the energy profile is calculated at $t_{Co} = 0.6$ nm, a single minimum is present around $R_s = 12$ nm ($R_s/R = 0.048$), see Figure 3d-e, and position of this minimum agrees with skyrmion stabilized without the use of frozen spins. The stabilization of this skyrmion is possible due to canceling of contributing forces: magnetostatic, exchange and anisotropy.[13] These forces are calculated from derivatives of contributions to the total energy with respect to the skyrmion radius R_s and are presented in Figure 3d as F_{mag} for magnetostatic force and F_σ for remaining forces. The sum of all forces ΣF presented in Figure 3e is zero at the energy minimum. The effect of the dot edge plays minor role on stabilization and this skyrmion state is also expected to exist in infinite film.[19] The skyrmion stabilization is realized due to the nonlinear change in the magnetic energy as function of skyrmion radius induced when the skyrmion diameter is in order of domain wall (DW) width.[14][2]

When the Co thickness is increased to $t_{Co} = 2.4$ nm, the skyrmions with two different sizes can be stable. The energy profile as function of the skyrmion radius is presented in Figure 3a. The energy minima correspond to skyrmion sizes found in Figure 3a at this value of t_{Co}. Analyzing the force F_{mag} (Figure 3f) one can observe significant curvature of the function at high values of R_s. The curvature increases with thickness (or M_s) increasing (Figure 3i) and appears due to presence of the nanodot edge. The edge changes the F_{mag} function and leads to stabilization of large radius skyrmion. Thus, presence of the lateral confinement modifies the magnetostatic energy introducing nonlinearity in the magnetostatic force F_{mag} as function of the skyrmion radius (see Figure 3f, i), and results in stabilization of skyrmion with size that is not related to the dot radius and DW width. The size of large skyrmion is not fixed to $R_s/R = 0.7$–0.8 as in Ref. [19], but is proportional to the magnetostatic interaction strength. The Co thickness 6.6 nm ($n = 11$) and $D = 1.4$–$1.6\,\mathrm{mJ\,m^{-2}}$ [11] correspond according to Figure 2a and c to the stable Néel skyrmion with the radius $R_s/R = 0.6$.

We distinguish two mechanisms of the skyrmion stabilization in nanodots: i) small radius Néel skyrmion is stabilized by DMI when R_s is in range of the DW width; and ii) large radius skyrmion is stabilized by nonlinear increase of the magnetostatic interaction with skyrmion radius increasing. The latter is solely present in confined geometries. The stabilization of these skyrmions is independent and a bifurcation can be present in some cases, leading to the skyrmion bi-stability in nanodots.

Further increase of t_{Co} leads to increase of curvature of the dependence $F_{mag}(R_s)$, crossing at small values of R_s is not possible and small radius skyrmion becomes unstable (Figure 3i). The effect of the nonlinearity in the magnetostatic energy is very pronounced and large radius skyrmion is still stable.

An example shown in Figure 3a for particular set of parameters exhibits a double well potential separated by small energy barrier, $\Delta E = 2.33 \times 10^{-20}$ J. The energy barrier height

[1] We assume that the the dot radius is much larger than the separation between the ferromagnetic layers $t_{sep} \ll R$ leading to uniform magnetic field across the thickness. We assume also that the effective dot thickness should be much smaller than the cycloid period, $t_{eff} \ll L$, where $L = 4\pi A/D$ and A being the micromagnetic exchange constant.[19]

[2] In nanodot, this nonlinearity in the energy as function of the skyrmion radius is also present when the difference between dot radius and skyrmion radius is in the range of domain wall width (or slightly higher due to spin canting at the dot boundaries). Thus, the stable skyrmions in nanodot can be classified as small or large size even when the magnetostatic interaction is taken into account as an effective easy-plane anisotropy.[19]

© 2017 WILEY-VCH Verlag GmbH & Co. KGaA, Weinheim

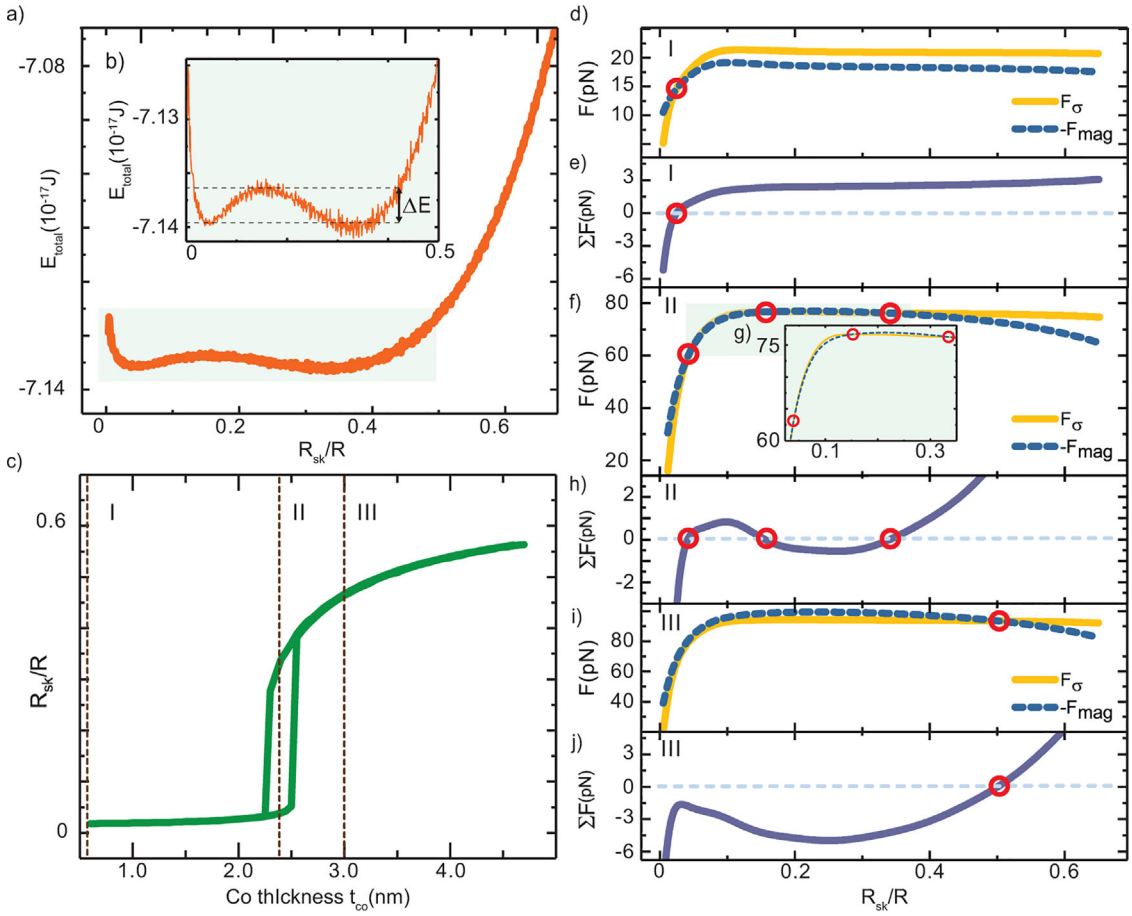

Figure 3. The energy profile of skyrmion state as function of normalized skyrmion radius R_s/R in 250nm radius dot ($t_{Co} = 2.4$ nm and $D = 0.95$ mJ m^{-2}). b) Inset: enlarged energy profile with the indicated scale of the total energy. c) Small and large skyrmion size as function of the thickness of Co layer. Dashed lines marked as I, II, III correspond to the force analysis presented in the panels (d-j). d,f,i) present the forces corresponding to the dot with different Co thicknesses, 0.6 nm (I), 2.4 nm (II), and 3.0 nm (III), respectively. F_{mag} is a magnetostatic force, and remaining forces are presented by F_σ. e,h,j) The sum of all forces is presented for I, II, and III cases, respectively, where zero value corresponds to the energy minimum. Red circles indicate energy minimum expressed as a crossing of the curves of partial forces. g) Inset: enlarged forces for (II).

can be enhanced and optimized via control of the magnetic parameters, geometry or external magnetic field. The switching between two skyrmion states can be realized, for example, by sweeping external magnetic field or applying a field pulse. Therefore, the skyrmion size hysteresis behavior can be realized without presence of a Bloch point as in switching between the skyrmions with opposite polarities.[6] The calculated skyrmion bi-stability is principally different from one calculated accounting DMI for magnetic vortices[31] because the latter is realized for different signs of D.

In conclusion, we analyzed influence of the magnetostatic interaction in circular multilayer nanodots on stability of the skyrmion magnetization configurations in ferromagnetic layers. We found that the skyrmions can be stabilized due to two different mechanisms, primary DMI or primary magnetostatic interaction leading to small and large size skyrmions, respectively. We found that these two kinds of the skyrmions can be stable simultaneously in the same nanodot. Thus, we demonstrated bi-stability of the skyrmion configurations with the same core polarities, but different sizes. The bi-stable skyrmions can be obtained in dots with realistic values of the dot sizes and the DMI strength, exchange and anisotropy parameters. Our results open a new route to design and develop a more efficient skyrmion memory, where information is coded as a skyrmion equilibrium size. The simulation approach based on the build-in Mumax function frozen spins is able to estimate the minimum energy path between two Néel skyrmions with different radii.

Computational Details

We performed finite-difference time-domain micromagnetic simulations with Mumax^3 solver[32] using a uniformly discretized grid with the cell size 0.5–1.0 nm × 0.5–1.0 nm × 0.6–4.2 nm. We used a set of parameters, which describes a multilayer thin film with a perpendicular magnetic anisotropy and DMI induced at the interfaces. We took the parameters measured for multilayer Pt/Co/Ir dot in Ref. [11]: saturation magnetization $M_s = 956$ kA m^{-1}, exchange stiffness $A = 10.0$ pJ m^{-1}, and perpendicular

© 2017 WILEY-VCH Verlag GmbH & Co. KGaA, Weinheim

magnetic anisotropy $K_u = 0.717\,\mathrm{MJ\,m^{-2}}$. They are distributed uniformly in 0.6 nm thick Co layer. Ultrathin Pt/Co/Ir dot total thickness below 2.4 can be realized experimentally.[11,12] To keep magnetostatic interactions between the layers we used air-gap separation instead of the nonmagnetic spacers since the interlayer exchange was neglected. Total thickness of one repeat was 2.4nm. In order to simulate multilayer stacks we used finite periodic boundary conditions.[32] Magnetization non-uniformity through the thickness was neglected. To overcome staircase effects resulting from the calculation method, we used built-in Mumax function edge smooth.

The calculations of skyrmion size dependence on the DMI strength were performed by starting from an artificially nucleated skyrmion magnetic configuration, relaxing system and measuring the skyrmion radius (if skyrmion was stable). We increased the interfacial DMI, equilibrated the system at every DMI step and used the previous magnetization configuration as an initial state in the subsequent DMI increase step. Next, the same procedure was repeated decreasing the DMI strength, starting from a large radius skyrmion at maximum DMI value possible.

We used frozen spins technique to calculate the skyrmion magnetic energy exploiting the Mumax built-in frozen spin function. The edge of the skyrmion ($m_z = 0$, $m_r = 1$) is defined as a narrow ring around the center of the nanodot. Such condition facilitates a Néel skyrmion configuration with radius corresponding to the radius of the ring. The rest of the spins are free and relax to an energy minimum. This method does not assume any shape of the skyrmion profile, only its radius, in contrast with the semi-analytical approach.[14,21] When varying the ring radius we obtain the total skyrmion energy as a function of its radius, see Figure 3.

Acknowledgements

The project is financed by SASPRO Program. The research was supported by the People Program (Marie Curie Actions) European Union's FP7 under REA grant agreement No. 609427 (project WEST 1244/02/01) and further co-funded by the Slovak Academy of Sciences and the European Union Horizon 2020 Research and Innovation Program under Marie Sklodowska-Curie grant agreement No. 644348. The financial assistance from the National Science Center of Poland (MagnoWa DEC-2012/07/E/ST3/00538) is also acknowledged. K.G. acknowledges support by IKERBASQUE (the Basque Foundation for Science), the Spanish MINECO grants FIS2016-78591-C3-3-R and MAT2013-47078-C2-1-P. The simulations were partially performed at the Poznan Supercomputing and Networking Center (Grant No. 209) and supported by the National Scholarship Program of the Slovak Republic funded by the Ministry of Education, Science, Research, and Sport of the Slovak Republic.

Conflict of Interest

The authors declare no conflict of interest.

Keywords

bi-stability, magnetostatic interactions, nanodots, Néel skyrmion, skyrmions

Received: August 4, 2017
Revised: August 30, 2017
Published online:

[1] I. Dzyaloshinsky, *J. Phys. Chem. Solids* **1958**, *4*, 241.
[2] T. Moriya, *Phys. Rev.* **1960**, *120*, 91.
[3] A. Fert, P. M. Levy, *Phys. Rev. Lett.* **1980**, *44*, 1538.
[4] A. Crépieux, C. Lacroix, *J. Magn. Magn. Mater.* **1998**, *182*, 341.
[5] A. O. Leonov, T. L. Monchesky, N. Romming, A. Kubetzka, A. N. Bogdanov, R. Wiesendanger, *New J. Phys.* **2016**, *18*, 1.
[6] M. Beg, R. Carey, W. Wang, D. Cortés-Ortuño, M. Vousden, M. A. Bisotti, M. Albert, D. Chernyshenko, O. Hovorka, R. L. Stamps, H. Fangohr, *Sci. Rep.* **2015**, *5*, 17137.
[7] G. Yu, P. Upadhyaya, Q. Shao, H. Wu, G. Yin, X. Li, C. He, W. Jiang, X. Han, P. K. Amiri, K. L. Wang, *Nano Lett.* **2017**, *17*, 261.
[8] A. Fert, V. Cros, J. Sampaio, *Nat. Nanotechnol.* **2013**, *8*, 152.
[9] N. S. Kiselev, a. N. Bogdanov, R. Schäfer, U. K. Rößler, *J. Phys. D: Appl. Phys.* **2011**, *44*, 392001.
[10] M. Mruczkiewicz, M. Krawczyk, K. Y. Guslienko, *Phys. Rev. B* **2017**, *95*, 094414.
[11] C. Moreau-Luchaire, C. Moutais, N. Reyren, J. Sampaio, C. A. F. Vaz, N. Van Horne, K. Bouzehouane, K. Garcia, C. Deranlot, P. Warnicke, P. Wohlhüter, J. M. George, M. Weigand, J. Raabe, V. Cros, A. Fert, *Nat. Nanotechnol.* **2016**, *11*, 444.
[12] S. D. Pollard, J. A. Garlow, J. Yu, Z. Wang, Y. Zhu, H. Yang, *Nat. Commun.* **2017**, *8*, 14761.
[13] O. Boulle, J. Vogel, H. Yang, S. Pizzini, D. d. S. Chaves, A. Locatelli, T. O. M. A. Sala, L. D. Buda-Prejbeanu, O. Klein, M. Belmeguenai, Y. Roussigné, A. Stashkevich, S. M. Chérif, L. Aballe, M. Foerster, M. Chshiev, S. Auffret, I. M. Miron, G. Gaudin, *Nat. Nanotechnol.* **2016**, *11*, 449.
[14] F. Büttner, I. Lemesh, G. S. D. Beach, arXiv:1704.08489, **2017**. https://arxiv.org/abs/1704.08489
[15] A. Bogdanov, A. Hubert, *J. Magn. Magn. Mater.* **1994**, *138*, 255.
[16] A. Fert, N. Reyren, V. Cros, *Nat. Rev. Mater.* **2017**, *2*, 17031.
[17] H. Du, W. Ning, M. Tian, Y. Zhang, *Phys. Rev. B* **2013**, *87*, 14401.
[18] H. Du, W. W. Ning, M. Tian, Y. Zhang, *EPL (Europhys. Lett.)* **2013**, *101*, 37001.
[19] S. Rohart, A. Thiaville, *Phys. Rev. B* **2013**, *88*, 184422.
[20] C. Moutafis, S. Komineas, C. A. F. Vaz, J. A. C. Bland, T. Shima, T. Seki, K. Takanashi, *Phys. Rev. B* **2007**, *76*, 104426.
[21] K. Y. Guslienko, *IEEE Magn. Lett.* **2015**, *6*, 4000104.
[22] K. Zeissler, M. Mruczkiewicz, S. Finizio, J. Raabe, P. M. Shepley, A. V. Sadovnikov, S. A. Nikitov, K. Fallon, S. McFadzean, S. McVitie, T. A. Moore, G. Burnell, C. H. Marrows, arXiv:1706.01065, **2017**. https://arxiv.org/abs/1706.01065
[23] M. A. Castro, S. Allende, *J. Magn. Magn. Mater.* **2016**, *417*, 344.
[24] A. O. Leonov, U. K. Rößler, M. Mostovoy, EPJ Web of Conferences *75*, 05002 (**2013**).
[25] R. Tomasello, E. Martinez, R. Zivieri, L. Torres, M. Carpentieri, G. Finocchio, *Sci. Rep.* **2014**, *4*, 6784.
[26] X. Yu, N. Kanazawa, W. Zhang, T. Nagai, T. Hara, K. Kimoto, Y. Matsui, Y. Onose, Y. Tokura, *Nat. Commun.* **2012**, *3*, 988.
[27] N. Vidal-Silva, A. Riveros, J. Escrig, *J. Magn. Magn. Mater.* **2017**, *443*, 116.
[28] W. Koshibae, N. Nagaosa, *Nat. Commun.* **2016**, *7*, 10542.
[29] K. Y. Guslienko, Z. V. Gareeva, *J. Magn. Magn. Mater.* **2017**, *442*, 176.
[30] J. Sampaio, V. Cros, S. Rohart, A. Thiaville, A. Fert, *Nat. Nanotechnol.* **2013**, *8*, 839.
[31] A. B. Butenko, A. A. Leonov, A. N. Bogdanov, U. K. Rößler, *Phys. Rev. B* **2009**, *80*, 1.
[32] A. Vansteenkiste, B. V. De Wiele, *J. Magn. Magn. Mater.* **2011**, *323*, 2585.

 © 2017 WILEY-VCH Verlag GmbH & Co. KGaA, Weinheim